Supporting Information

Highly Stable and Luminescent Perovskite-Polymer Composites from a Convenient and Universal Strategy

Yumeng Xin[1], *Hongjie Zhao*[2], *Jiuyang Zhang*[1]*

[1]School of Chemistry and Chemical Engineering, Southeast University, Nanjing, 211189, PR China

[2]School of Chemical Engineering & Technology, China University of Mining and Technology, Xuzhou, 221116, PR China

Corresponding Authors

*E-mail: jiuyang@seu.edu.cn

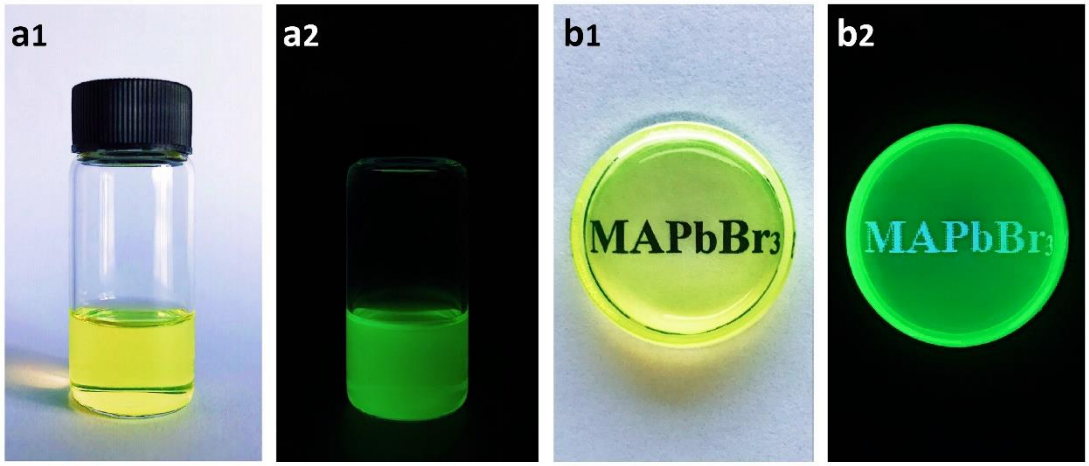

Figure S1. Photos in room light (a1) and in UV-illumination (a2) of methylammonium lead bromide nanoparticles ($MAPbBr_3$) in bulk MMA; the photos of the polymerized $MAPbBr_3$-PMMA taken under room light (b1) and UV-illumination (b2).

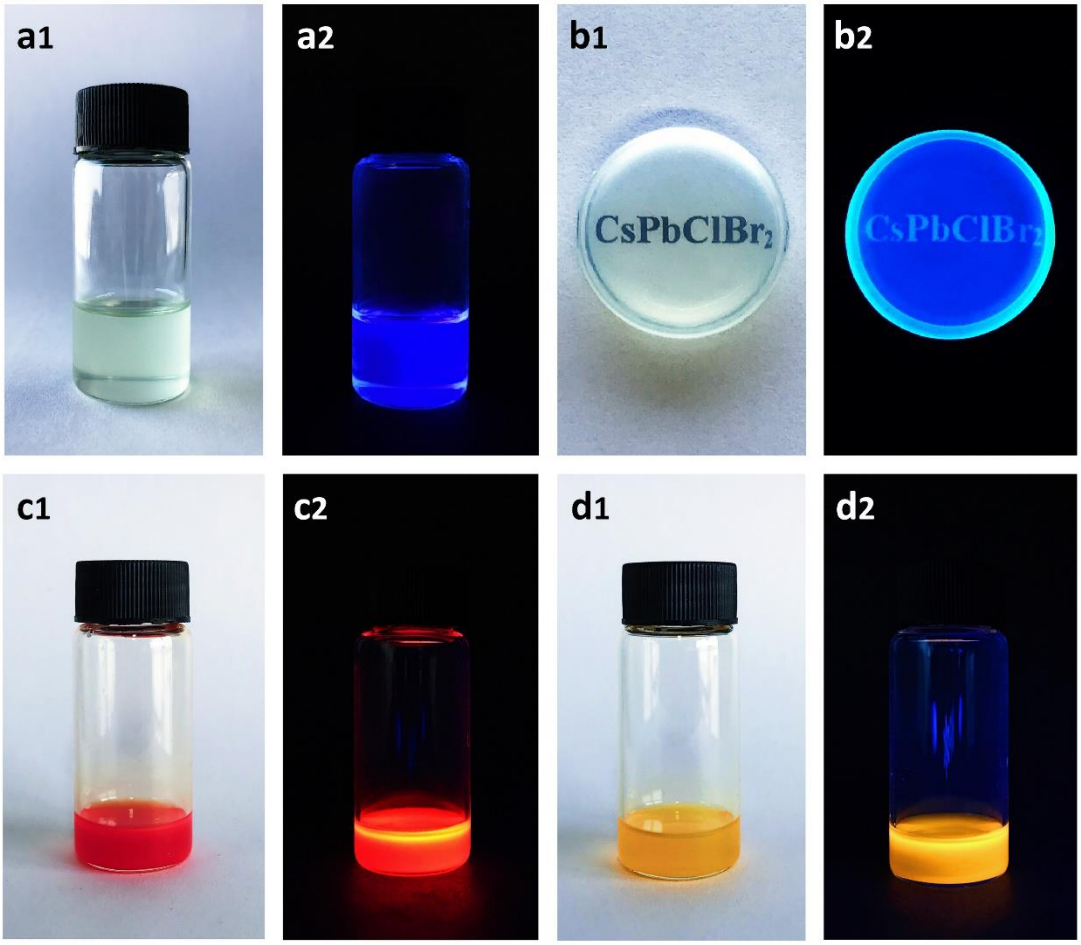

Figure S2. Photos in room light (a1) and UV-illumination (a2) of $CsPbClBr_2$ inorganic perovskite quantum dots formed in bulk MMA; photos of disks (diameter: 3 cm) from $CsPbClBr_2$-PMMA composite under ambient room light (b1) and UV illumination (b2). Photos in room light (c1) and in UV-illumination (c2) of $CsPbBr_{1.2}I_{1.8}$ inorganic perovskite quantum dots formed in toluene; the photos of $CsPbBr_{1.2}I_{1.8}$ inorganic perovskite quantum dots formed in bulk MMA solution taken under room light (d1) and UV-illumination (d2).

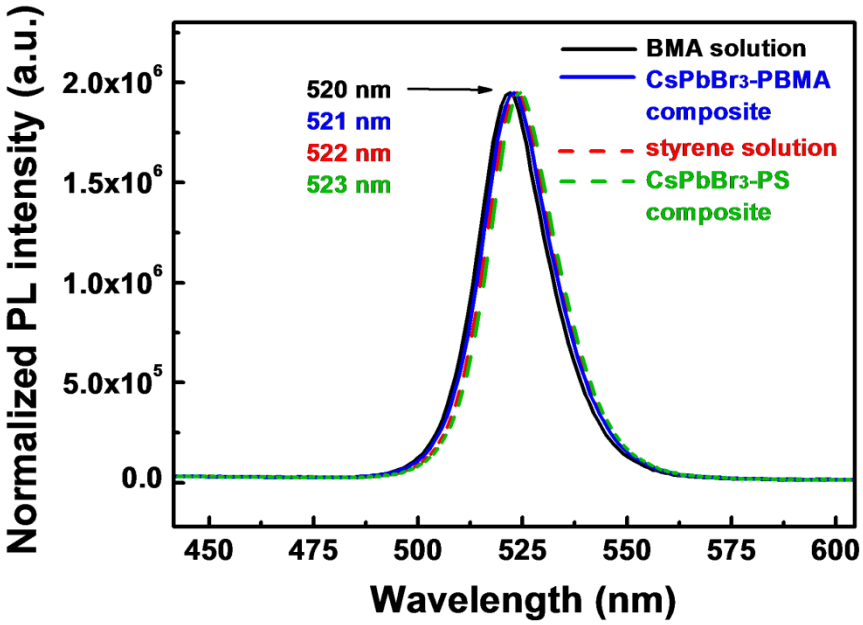

Figure S3. Normalized PL spectra of emissive bulk BMA/styrene solution and the resulted $CsPbBr_3$-PBMA/$CsPbBr_3$-PS composite.

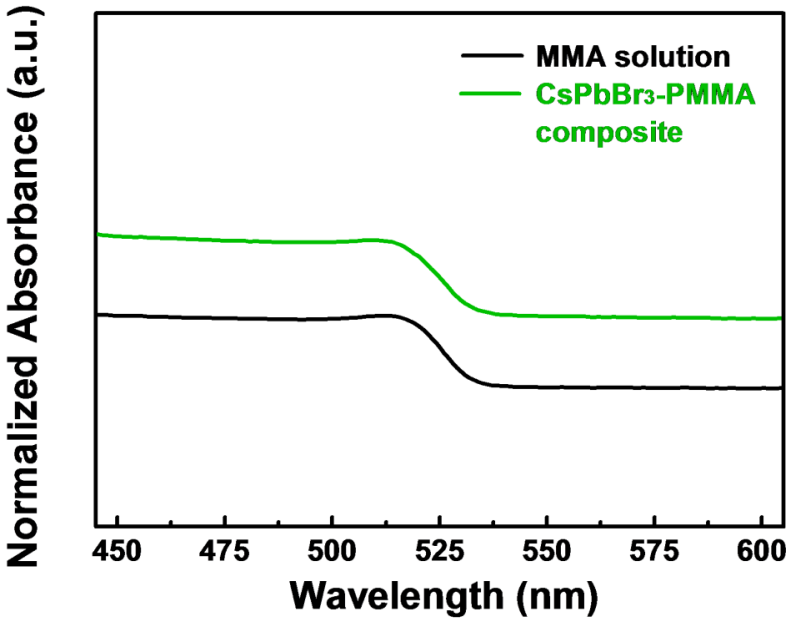

Figure S4. Normalized absorption spectra of emissive bulk MMA solution and the resulted $CsPbBr_3$-PMMA composite.

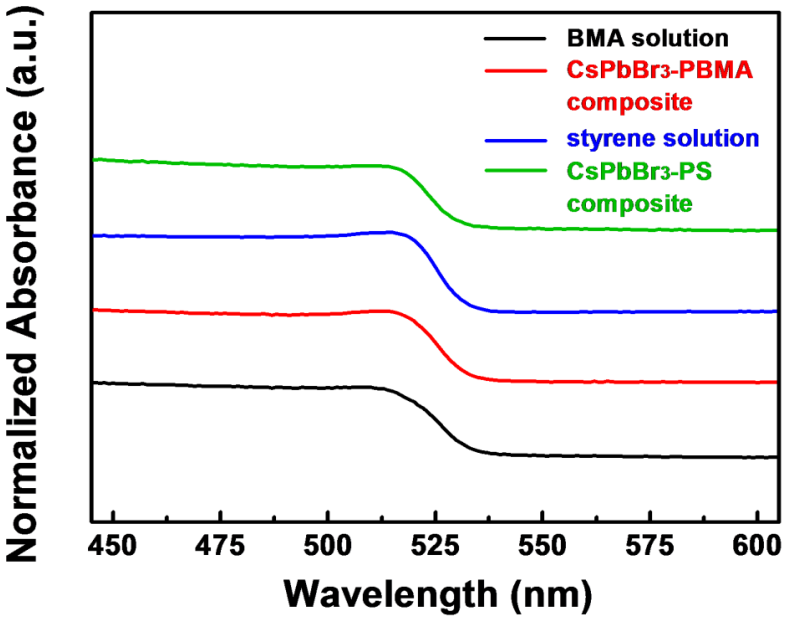

Figure S5. Normalized absorption spectra of emissive bulk BMA/styrene solution and the resulted $CsPbBr_3$-PBMA/$CsPbBr_3$-PS composite.

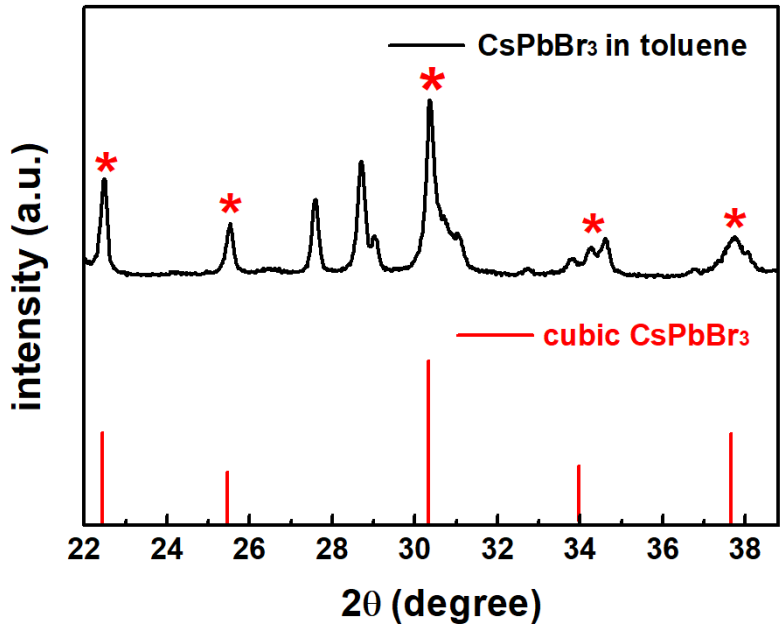

Figure S6. X-ray diffraction (XRD) patterns of $CsPbBr_3$ crystals obtained from toluene. The pattern is the same as $CsPbBr_3$ crystals obtained from MMA, indicating no small molecules of MMA incorporating into crystals.

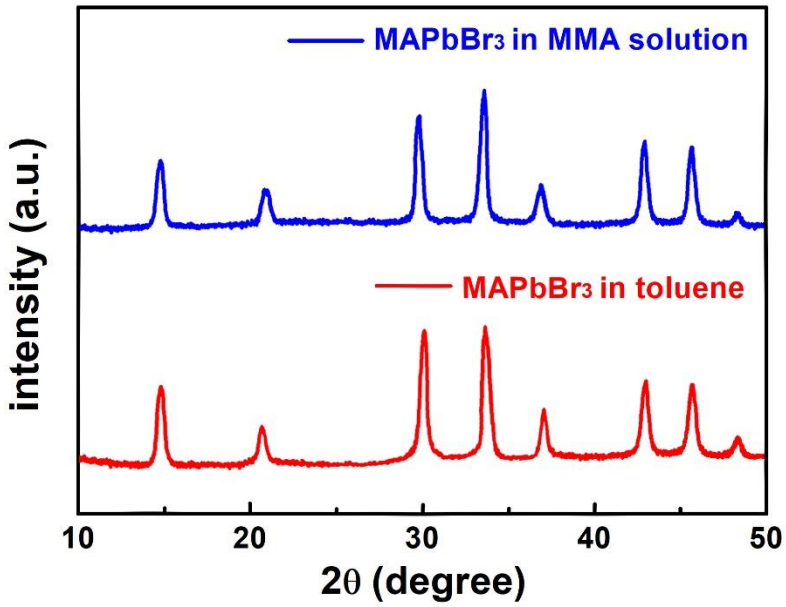

Figure S7. X-ray diffraction (XRD) patterns of $MAPbBr_3$ crystals obtained from emissive bulk MMA solution and toluene. No obvious change was observed of crystals from MMA and toluene.

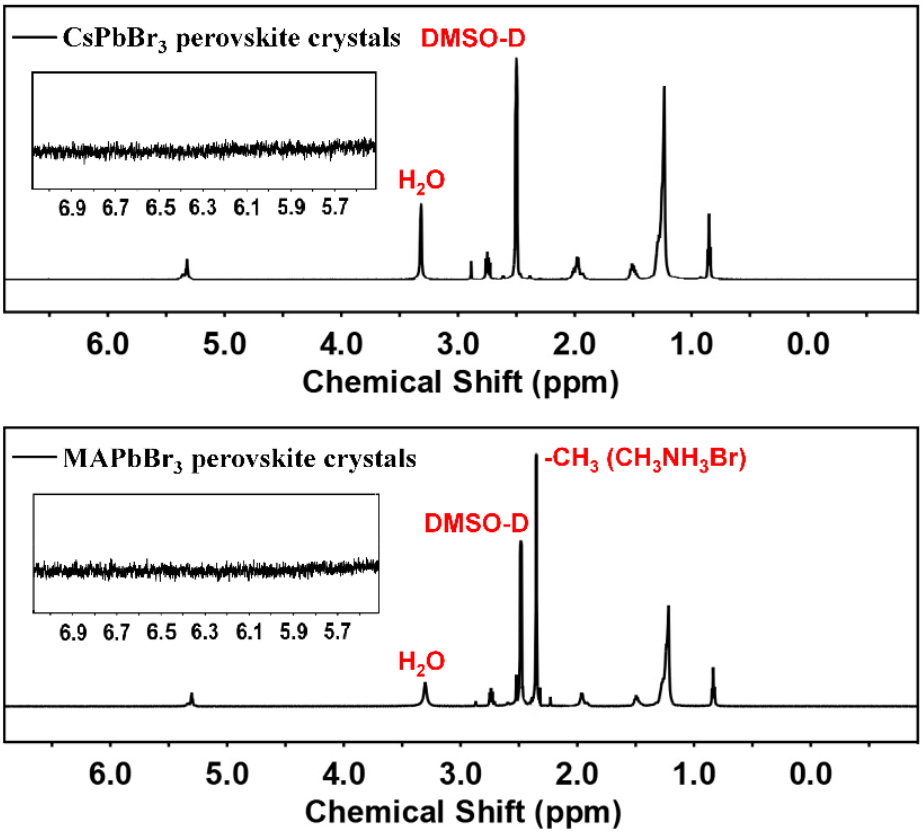

Figure S8. ^{1}H NMR spectra of $CsPbBr_3$ and $MAPbBr_3$ perovskite crystals (The inset is the zoom-in spectrum displaying signals from 6.0 to 0.0 ppm). No peaks residual MMA monomer observed in the ^{1}H NMR spectra (the signals in spectra were attributed to the oleylamine, oleic acid and methyl of CH_3NH_3Br, without the signals of MMA monomer.), showing that MMA did not exist in the final crystals.

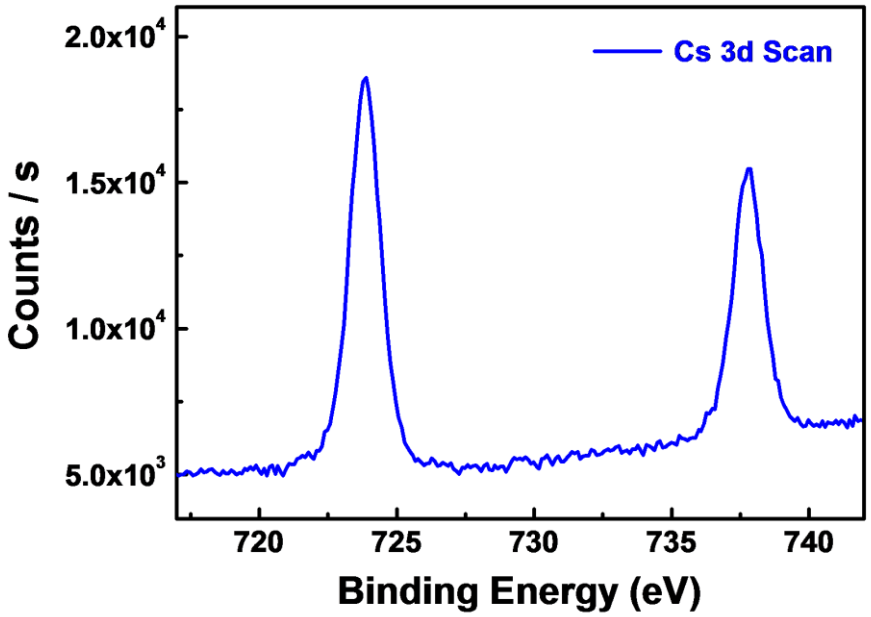

Figure S9. X-ray photoelectron spectroscopy of the Cs element in the resulted $CsPbBr_3$-PMMA composite.

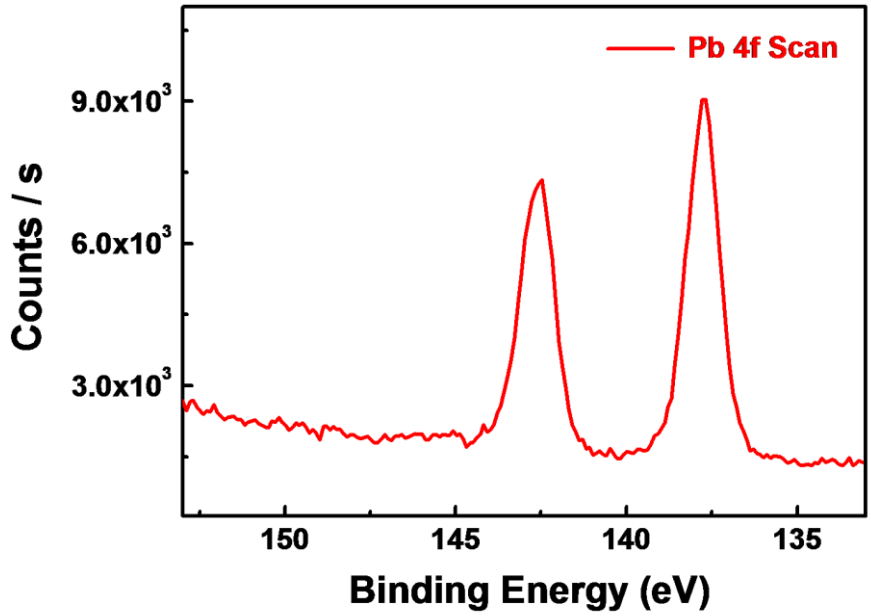

Figure S10. X-ray photoelectron spectroscopy of the Pb element in the resulted $CsPbBr_3$-PMMA composite.

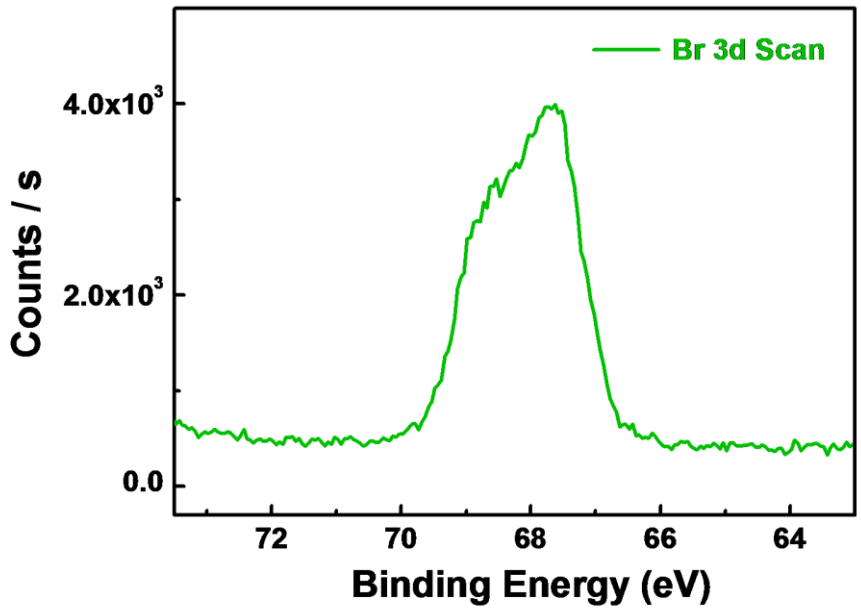

Figure S11. X-ray photoelectron spectroscopy of the Br element in the resulted $CsPbBr_3$-PMMA composite. Weak peaks were observed due to the very small weight fraction of $CsPbBr_3$ in polymers.

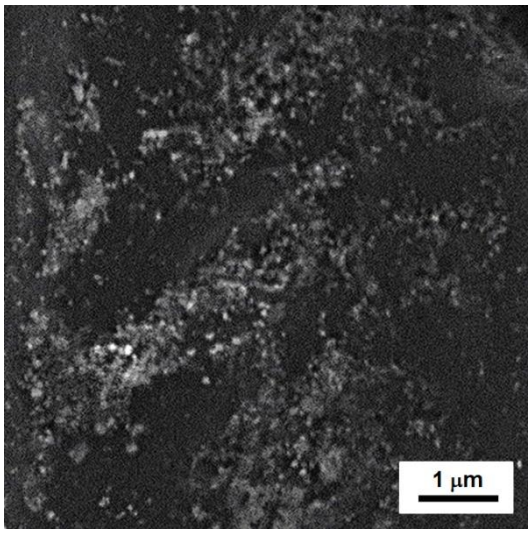

Figure S12. Cross-section scanning electron microscope (SEM) image for the resulted $CsPbBr_3$-PMMA composite with high content of $CsPbBr_3$ crystals (100 μL of the precursor solution was added into the mixture of solution with MMA (1.5 mL), EDMA (28 μL) and TPO (5.19 mg)).

Table S1. Photoluminescence quantum yields (PLQYs) of the resulted $CsPbBr_3$-PMMA composite (10-50 nm) and the resulted $CsPbBr_3$-PMMA composite with large $CsPbBr_3$ particles (10-150 nm). The large size of $CsPbBr_3$ particles were prepared by adding 100 μL of the precursor solution into the mixture of solution with MMA, EDMA and TPO.

PLQYs	$CsPbBr_3$ Particles (10−50 nm)	$CsPbBr_3$ Particles (10−150 nm)
The resulted $CsPbBr_3$-PMMA composite	54.6%	43.5%

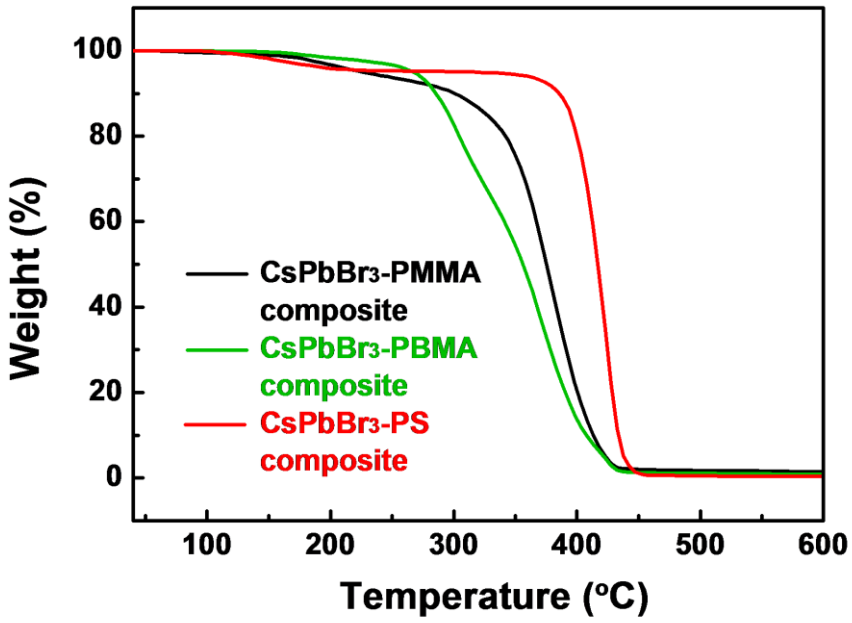

Figure S13. Thermal gravimetric analysis (TGA) curves of the resulted $CsPbBr_3$-PMMA, $CsPbBr_3$-PBMA and $CsPbBr_3$-PS composite at a heating rate of 10 ℃ min^{-1} in N_2.

Table S2. Photoluminescence quantum yields (PLQYs) of the resulted $CsPbBr_3$-PMMA, $CsPbBr_3$-PBMA and $CsPbBr_3$-PS composite.

PLQYs	PMMA	PBMA	PS
Thermal polymerized $CsPbBr_3$-polymer composite	7.3%	9.2%	0.7%
UV-polymerized $CsPbBr_3$-polymer composite	54.6%	62.2%	–[a)]

a) UV-polymerized $CsPbBr_3$-PS composite was not formed due to the low polymerization constant of styrene.

Table S3. Photoluminescence quantum yields (PLQYs) of the $CsPbBr_3$ crystals without TPO, $CsPbBr_3$ with TPO and $CsPbBr_3$ with TPO (under the UV-light for 1 h) in toluene (50 μL of the precursor solution was added into the mixture of solution with toluene (1.5 mL) and TPO (5.19 mg)).

PLQYs	Without TPO	With TPO	With TPO (under the UV-light)
$CsPbBr_3$ crystals in toluene	64.6%	62.2%	54.7%

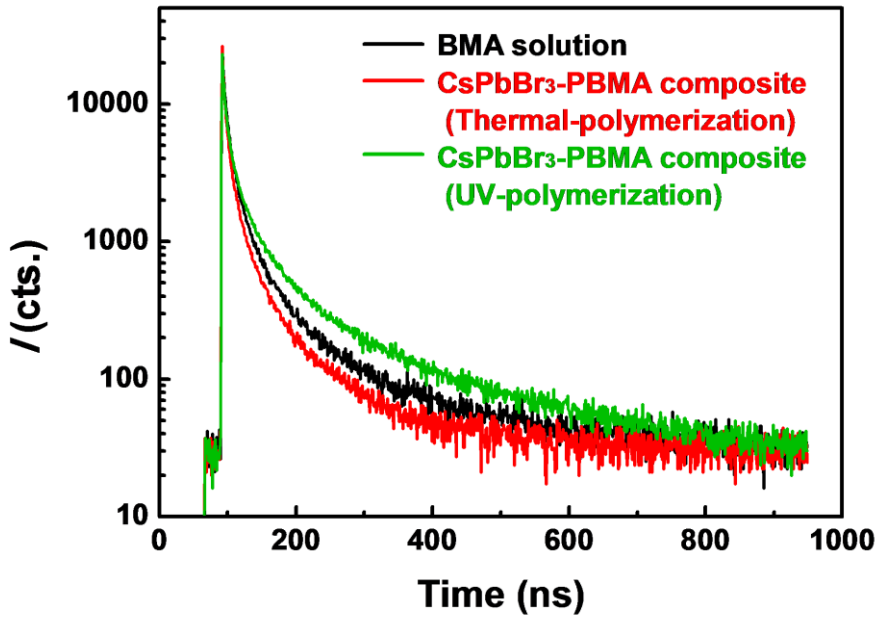

Figure S14. Time-resolved PL decays and fitting curves of emissive bulk BMA solutions and the resulted $CsPbBr_3$-PBMA composite.

Table S4. Triexponential fitting results of emissive bulk MMA solution and the resulted $CsPbBr_3$-PMMA composite.

Sample	MMA solution	Thermal polymerized $CsPbBr_3$-PMMA composite	UV-polymerized $CsPbBr_3$-PMMA composite
A_1 [a]	1.35×10^6	2.68×10^5	5.71×10^5
τ_1 (ns) [b]	3.0	3.0	3.5
A_2 [a]	1.76×10^6	4.19×10^5	6.47×10^5
τ_2 (ns) [b]	16	21.7	20.6
τ_{avg} (ns) [c]	14.4	20.2	18.4

Time-resolved PL decay curves were fitted by a diexponential (eqs 1 and 2) function.

[a] A_1 and A_2 represents weight, [$A(t) = A_0 + A_1\exp-(t-t_0)/\tau_1 + A_2\exp-(t-t_0)/\tau_2$ (eqs 1)] ; [b] τ_1 and τ_2 represents PL lifetime; [c] The average lifetime were calculated using [$\tau_{avg} = (A_1\tau_1^2 + A_1\tau_1^2)/(A_1\tau_1 + A_1\tau_1)$ (eqs 2)].

Table S5. Triexponential fitting results of emissive bulk BMA solution and the resulted $CsPbBr_3$-PBMA composite.

Sample	BMA solution	Thermal polymerized $CsPbBr_3$-PBMA composite	UV-polymerized $CsPbBr_3$-PBMA composite
A_1 [a)]	4.32×10^5	1.27×10^6	1.92×10^4
τ_1 (ns) [b)]	3.9	3.0	4.0
A_2 [a)]	2.23×10^5	1.41×10^6	7.74×10^4
τ_2 (ns) [b)]	25.6	18.2	35.4
τ_{avg} (ns) [c)]	20.7	16.2	34.5

Time-resolved PL decay curves were fitted by a diexponential (eqs 1 and 2) function.

[a)] A_1 and A_2 represents weight, [$A(t) = A_0 + A_1\exp-(t-t_0)/\tau_1 + A_2\exp-(t-t_0)/\tau_2$ (eqs 1)] ; [b)] τ_1 and τ_2 represents PL lifetime; [c)] The average lifetime were calculated using [$\tau_{avg} = (A_1\tau_1^2 + A_1\tau_1^2)/(A_1\tau_1 + A_1\tau_1)$ (eqs 2)].

Table S6. Triexponential fitting results of emissive bulk styrene solution and the resulted $CsPbBr_3$-PS composite.

Sample	Styrene solution	Thermal polymerized $CsPbBr_3$-PS composite
A_1 [a)]	9.14×10^4	2.143×10^6
τ_1 (ns) [b)]	5.2	4.5
A_2 [a)]	6.33×10^4	1.76×10^6
τ_2 (ns) [b)]	37.9	17.8
τ_{avg} (ns) [c)]	32.5	14.7

Time-resolved PL decay curves were fitted by a diexponential (eqs 1 and 2) function.

[a)] A_1 and A_2 represents weight, [$A(t) = A_0 + A_1\exp-(t-t_0)/\tau_1 + A_2\exp-(t-t_0)/\tau_2$ (eqs 1)] ; [b)] τ_1 and τ_2 represents PL lifetime; [c)] The average lifetime were calculated using[$\tau_{avg} = (A_1\tau_1^2 + A_1\tau_1^2)/(A_1\tau_1 + A_1\tau_1)$ (eqs 2)].

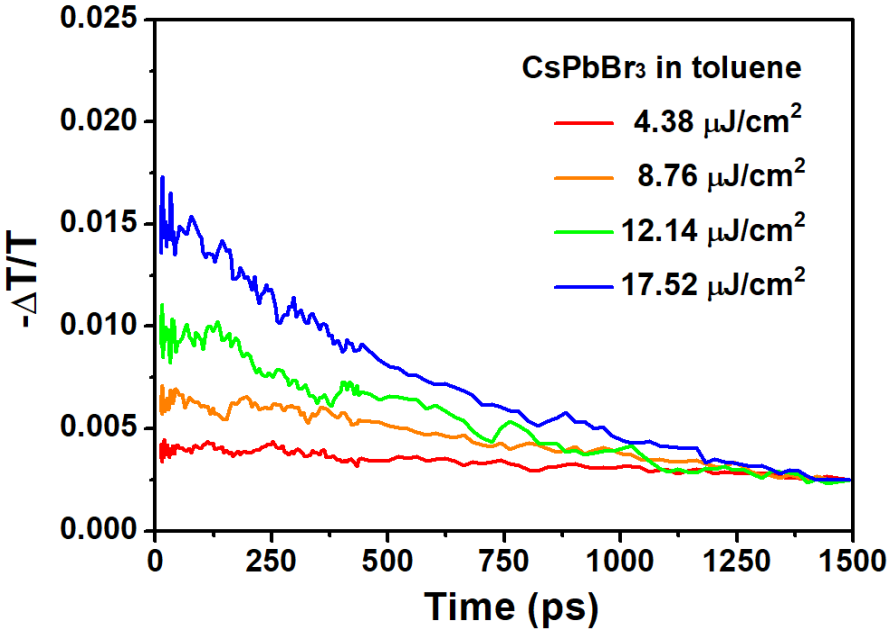

Figure S15. TA spectra of $CsPbBr_3$ in toluene.

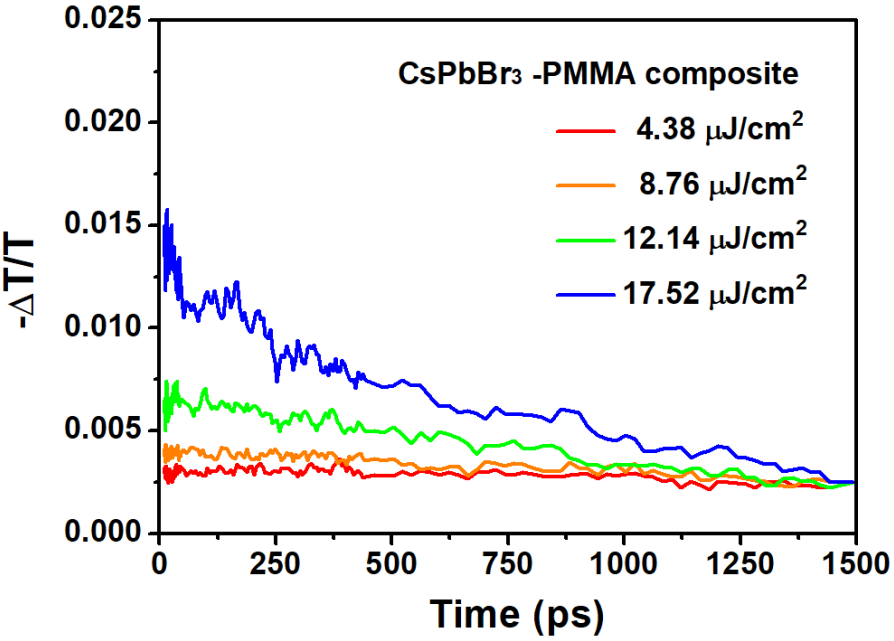

Figure S16. TA spectra of the resulted $CsPbBr_3$-PMMA composite.

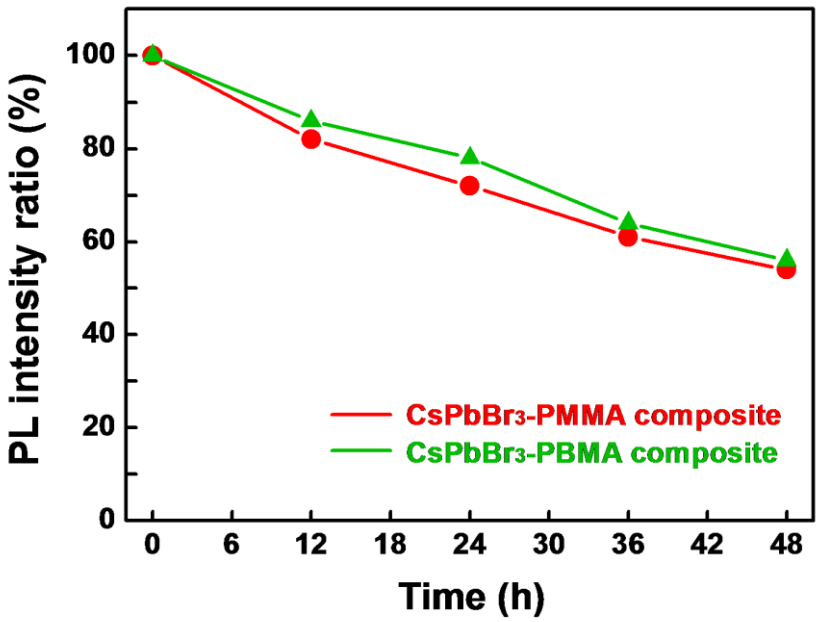

Figure S17. Time-dependent PL intensity of $CsPbBr_3$-PMMA and $CsPbBr_3$-PBMA composites in water.

Table S7. Photoluminescence quantum yields (PLQYs) of the resulted $CsPbBr_3$-PMMA composite and $MAPbBr_3$-PMMA composite before or after heated to 80 ℃ and kept at this temperature for 24 h in nitrogen atmosphere.

PLQYs	Before heated	After heated
The resulted $CsPbBr_3$-PMMA composite	62.4%	51.6%
The resulted $MAPbBr_3$-PMMA composite	49.8%	46.5%

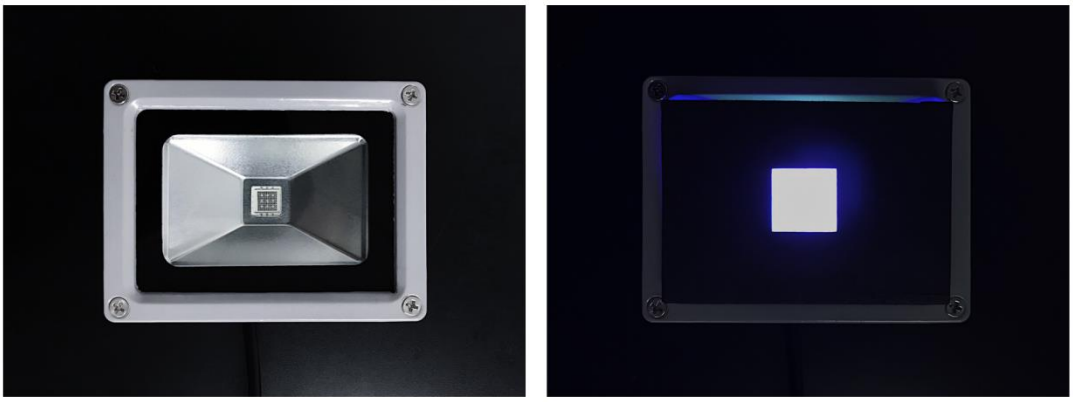

Figure S18. Photos are taken under ambient room light of blue LED (left) and white LED (right).

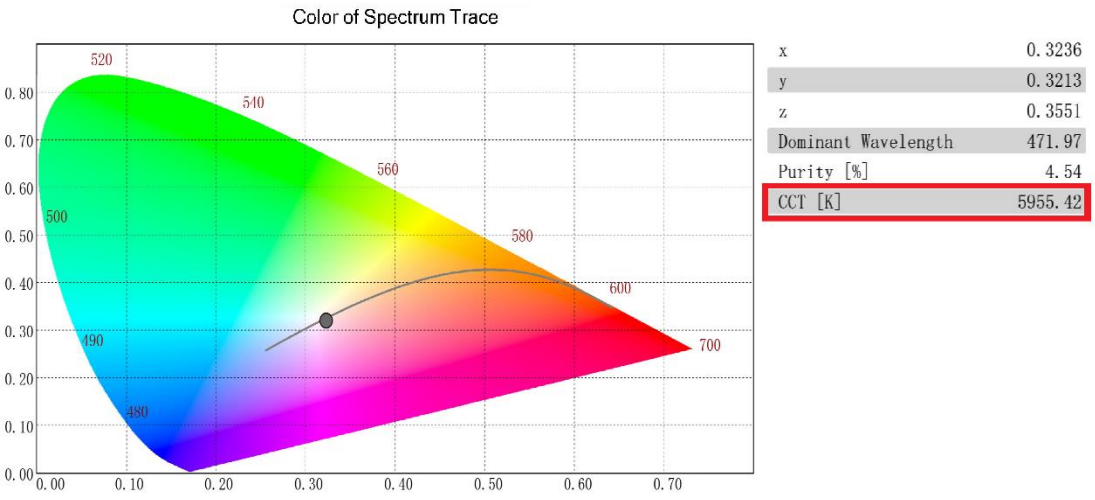

Figure S19. The color coordinates (gray dot) of obtained white LED in CIE diagram.

The color temperature (CCT) of the white LED was achieved at 5955.42 K.

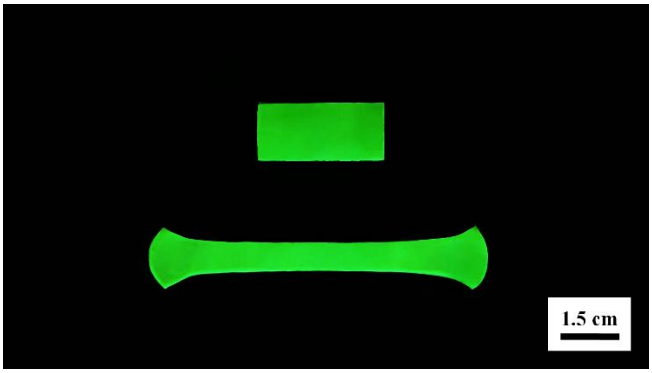

Figure S20. The photos of the resulted $CsPbBr_3$-PBMA composite before (top) and after stretching (down) under UV-illumination.

Table S8. Photoluminescence quantum yields (PLQYs) of the resulted $CsPbBr_3$-PMMA composite and the resulted $CsPbBr_3$-PMMA composite with high content of $CsPbBr_3$ crystals.

PLQYs	**Standard content of $CsPbBr_3$ crystals**	**High content of $CsPbBr_3$ crystals**
The resulted $CsPbBr_3$-PMMA composite	54.6%	43.5%

Table S9. Comparison of this work with other current correlative research.

Emitter Type	PL_{max} (nm)	Synthetic condition [a)]	$PLQY_{max}$ in polymer martix	Ref.
$CsPbBr_3$ NCs	521	Air; RT; In bulk monomers	62.2%	This work
$MAPbBr_{3-x}Cl_x$ NCs	505	Air; RT; DMF and toulene	56%	[1]
$CsPbBr_3$ NCs	513	Ar; 120 ^oC; ODE	53%	[2]
$MAPbBr_3$ NPs	530	RT; DMF	48%	[3]
$FAPbBr_3$ NPs	530	Air; RT; DMF, butanol and toluene	30%	[4]
$MAPbBr_3$ NPs	527	Air; 80 ^oC; DMF and ODE	23%	[5]
$MAPbBr_3$ amorphous NPs	505	Air; RT; butyrolactone and DMF	3.8%	[6]

[a)] Synthetic condition include whether usage of insert gas ,the synthetic temperature and solvent.

Abbreviations: Argon atmosphere (Ar); methylammonium cation (MA); formamidinium (FA); nanocrystals (NCs); nanoparticles (NPs); room temperature (RT); octadecene (ODE); dimethyl formamide (DMF).

References

[1] Sun, H.; Yang, Z. Y.; Wei, M. Y.; Sun, W.; Li, X. Y.; Ye, S. Y.; Zhao, Y. B.; Tan, H. R.; Kynaston, E. L.; Schon, T. B.; Yan, H.; Lu, Z. H.; Ozin, G. A.; Sargent, E. H.; Seferos, D. S. Chemically Addressable Perovskite Nanocrystals for Light-Emitting Applications. *Adv. Mater.* **2017**, *29*, 17001153.

[2] Meyns, M.; Peralvarez, M.; Heuer-Jungemann, A.; Hertog, W.; Ibanez, M.; Nafria, R.; Genc, A.; Arbiol, J.; Kovalenko, M. V.; Carreras, J.; Cabot, A.; Kanaras, A. G. Polymer-Enhanced Stability of Inorganic Perovskite Nanocrystals and Their Application in Color Conversion LEDs. *ACS Appl. Mat. Interfaces* **2016**, *8*, 19579-19586.

[3] Wang, Y. N.; He, J.; Chen, H.; Chen, J. S.; Zhu, R. D.; Ma, P.; Towers, A.; Lin, Y.; Gesquiere, A. J.; Wu, S. T.; Dong, Y. J. Ultrastable, Highly Luminescent Organic–Inorganic Perovskite–Polymer Composite Films. *Adv. Mater.* **2016**, *28*, 10710-10717.

[4] Perumal, A.; Shendre1, S.; Li, M.; Eugene Tay,Y. K.; Sharma,V. K.; Chen,S.; Wei, Z.; Liu, Q.; Gao, Y.; Buenconsejo, P. J. S.; Tan, S. T.; Gan, C. L.; Xiong, Q.; Sum, T. C.; Demir, H. V. Specific Cell Surface Labeling of GPCRs using Split GFP. *Sci. Reports*, **2016**, DOI: 10.1038/srep36733.

[5] Schmidt, L. C.; Pertegas, A.; Gonzalez-Carrero, A.; Malinkiewicz, O.; Agouram, S.; Espallargas, G. M.; Bolink, H. J.; Galian, R. E.; Perez-Prieto, J. Nontemplate Synthesis of $CH_3NH_3PbBr_3$ Perovskite Nanoparticles. *J. Am. Chem. Soc.* **2014**, *136*, 850-853.

[6] Xing, J.; Yan, F.; Zhao, Y.; Chen, S.; Yu, H.; Zhang, Q.; Zeng, R.; Demir, H. V.; Sun, X.; Huan, A.; Xiong, Q. High-Efficiency Light-Emitting Diodes of Organometal Halide Perovskite Amorphous Nanoparticles. *ACS Nano* **2016**, *10*, 6623-6630.